Succinate accumulation drives ischaemia-reperfusion injury during organ transplantation

Jack L. Martin[1,6], Ana S. H. Costa[2,6], Anja V. Gruszczyk [1,3], Timothy E. Beach [1], Fay M. Allen[3], Hiran A. Prag[3], Elizabeth C. Hinchy[3], Krishnaa Mahbubani[1], Mazin Hamed[1], Laura Tronci[2], Efterpi Nikitopoulou[2], Andrew M. James [3], Thomas Krieg[4], Alan J. Robinson[3], Margaret H. Huang[1,3], Stuart T. Caldwell[5], Angela Logan[3], Laura Pala[5], Richard C. Hartley[5], Christian Frezza[2], Kourosh Saeb-Parsy[1, 7, *] and Michael P. Murphy[3, 4, 7, *]

[1]Department of Surgery and Cambridge NIHR Biomedical Research Centre, Biomedical Campus, University of Cambridge, Cambridge, CB2 2QQ, UK.

[2]MRC Cancer Unit, University of Cambridge, Hutchison/MRC Research Centre, Box 197, Cambridge Biomedical Campus, Cambridge, CB2 0XZ, UK

[3]MRC Mitochondrial Biology Unit, Biomedical Campus, University of Cambridge, Cambridge CB2 0XY, UK

[4] Department of Medicine, University of Cambridge, Cambridge, CB2 0QQ, UK

[5]School of Chemistry, University of Glasgow, Glasgow, G12 8QQ, UK

[6]These authors contributed equally: Jack L. Martin, Ana S. H. Costa.

[7]These authors contributed equally: Michael P. Murphy, Kourosh Saeb-Parsy

*Correspondence:

Professor Michael P. Murphy: mpm@mrc-mbu.cam.ac.uk

Phone: +44 1223 252900

Dr Kourosh Saeb-Parsy: ks10014@cam.ac.uk

Phone: +44 1223 336979

During heart transplantation, storage in cold preservation solution is thought to protect the organ by slowing metabolism; by providing osmotic support; and by minimising ischaemia-reperfusion (IR) injury upon transplantation into the recipient[1,2]. Despite its widespread use our understanding of the metabolic changes prevented by cold storage and how warm ischaemia leads to damage is surprisingly poor. Here, we compare the metabolic changes during warm ischaemia (WI) and cold ischaemia (CI) in hearts from mouse, pig, and human. We identify common metabolic alterations during WI and those affected by CI, thereby elucidating mechanisms underlying the benefits of CI, and how WI causes damage. Succinate accumulation is a major feature within ischaemic hearts across species, and CI slows succinate generation, thereby reducing tissue damage upon reperfusion caused by the production of mitochondrial reactive oxygen species (ROS)[3,4]. Importantly, the inevitable periods of WI during organ procurement lead to the accumulation of damaging levels of succinate during transplantation, despite cooling organs as rapidly as possible. This damage is ameliorated by metabolic inhibitors that prevent succinate accumulation and oxidation. Our findings suggest how WI and CI contribute to transplant outcome and indicate new therapies for improving the quality of transplanted organs.

Hearts are transplanted following donation after brainstem death (DBD), or following donation after circulatory death (DCD)[5-8]. Cooling the heart at the onset of ischaemia remains the mainstay of organ preservation, although emerging technologies allow preservation of some organs under normothermic and/or normoxemic conditions[8,9]. Rapid cooling minimises periods of WI during transplantation, which causes primary graft non-function, delayed or poor initial graft function, or chronic graft dysfunction[10,11]. Here we investigated the metabolic alterations during WI that contribute to tissue injury upon transplantation and which are prevented by CI.

We compared the metabolic profile of mouse hearts and in sections of pig and human myocardium under conditions that mimic cold organ storage during transplantation (CI; ~2˚C) and compared these with WI (37˚C) (Fig. 1a) over time. There was a much faster decline in ATP/ADP ratio during WI compared to CI in all three species (Fig. 1b-d), decreasing by over 50% during the first 5 min of WI while 5 min of

CI had a negligible effect. In CI heart contraction ceased within ~1–2 s, but in WI contraction continued for ~90 s, however ATP consumption by contraction during WI did not contribute to changes in ATP/ADP as preventing contraction by cardioplegia did not affect the ATP/ADP ratio (Supplementary Fig. 1a). The total amount of ATP and ADP (ΣATP + ADP) was also better maintained during CI than WI (Figs. 1e-g), while AMP accumulation was faster during WI than in CI (Supplementary Fig. 1b). Thus, CI preserves the tissue ATP/ADP ratio and slows the loss of adenine nucleotides.

During ischaemia oxidative phosphorylation stops and glucose is no longer delivered by the blood, hence the ATP/ADP ratio is sustained by glycogen-fuelled glycolysis[12], generating lactate (Supplementary Fig. 2a). Glycogen in the mouse and pig was more rapidly depleted during WI, but depletion halted, despite 20–25 % of the glycogen remaining (Supplementary Figs. 2b,c). During CI glycogen depletion was slower, but continued until all the glycogen was consumed (Supplementary Figs. 2b,c). During WI lactate initially accumulated but then plateaued, whereas during CI the rate of lactate build up was far slower, but continued throughout CI (Supplementary Figs. 2d-h). In the mouse lactate accumulation ceased when glycogen breakdown stopped (dashed red line; Supplementary Figs. 2b,d). The lactate/pyruvate and NADH/NAD^+ ion intensity ratios both increased far more rapidly and extensively during WI than during CI in the mouse (Supplementary Figs. 2h,i). Measurement of glycolytic intermediates in the mouse heart showed an accumulation of the GAPDH substrate glyceraldehyde-3-phosphate during WI, but the loss of products downstream of 3-phosphoglycerate kinase, 3-phosphoglycerate and phosphoenolpyruvate compared to CI (Supplementary Fig. 3). These two enzymes utilise NAD^+ and ADP and thus are likely inhibited by an elevated NADH/NAD^+ ratio and depletion of ADP (Supplementary Fig. 2a). This may slow glycolysis during WI, even though glycogen stores remain. Thus, during WI there was rapid glycogen depletion to drive glycolysis, which was slowed by CI.

To assess ischaemic metabolism more broadly, we performed a liquid chromatography/mass spectrometry (LC/MS)-based metabolomics analysis of mouse, pig and human heart tissue at various times under CI and WI (Supplementary Data 1a-c). Fifty-four metabolites were detected ubiquitously at up to 30 min WI and 480 min CI and changes in their abundance are presented as a heat map, demonstrating a similar overall

profile in mouse, pig and human heart tissue (Supplementary Fig. 4). We expanded the metabolome coverage to 107 metabolites for the mouse samples by a second LC/MS analysis which generated an extended heat map (Supplementary Fig. 5).

To compare how these metabolites changed between WI and CI (Supplementary Data 2) we generated volcano plots for mouse, pig and human heart tissue (Figs. 2a-c). Strikingly, most of the significant metabolic changes between WI and CI at the 30-min time point were comparable between mouse, pig and human hearts (red and green symbols). The only metabolites that changed in qualitatively different ways between species were fumarate and malate (Supplementary Data 1), which both accumulated during WI in the pig, decreased in the mouse and showed minor changes in the human. As can be seen there were notable and similar changes in many metabolites for all three species, including for choline, nicotinamide, alanine, proline, aconitate, branched chain amino acids and in the breakdown products of purines and pyrimidines.

Succinate increased dramatically during WI in all species (Figs. 2a-c). This finding was of particular interest because succinate accumulation during ischaemia contributes to IR injury upon reperfusion via generation of ROS by reverse electron transport (RET) at mitochondrial complex I[3,4]. Quantification of succinate levels over time showed that during WI there was rapid succinate accumulation within 6 min that increased further and plateaued at about 30 min (Figs. 3a–c). During CI succinate accumulation was far less, and even after 4h CI — the storage limit for human hearts to be transplanted — succinate was less than after 6 min WI (Figs. 3a-c). Even after extending CI of mouse hearts to 12 h the succinate level was still similar to that after 12 min of WI (Fig. 3d). The relative changes (Figs. 3a-c) as well as the absolute succinate levels (Fig. 3e) were remarkably similar in mouse, pig and human heart tissue. Cardioplegia slightly decreased succinate levels during WI in the mouse hearts (Supplementary Fig. 6a), but even so the relative accumulation was still 4 –5-fold above CI levels, suggesting that succinate accumulation is unrelated to changes in muscle contraction. As succinate accumulation is driven by the interconversion of fumarate and succinate by succinate dehydrogenase (SDH) we next assessed the succinate/fumarate ion intensity ratio (Figs. 3f-h). This showed a significant increase during WI in mouse, with a less pronounced increase in pig and human, that in all cases were slowed by CI. We

conclude that there is a significant accumulation of succinate during WI in mouse, pig and human hearts that is greatly slowed by cooling.

Succinate accumulation in ischaemic mouse hearts was proportional to temperature (Supplementary Fig. 6b). When a mouse heart was transferred to cold static storage its temperature dropped to ~2˚C within 1 min (Supplementary Fig. 6c), likely minimising succinate accumulation. However, the much larger human heart (~300 g vs ~150 mg for the mouse) will take far longer to cool during transplantation, potentially leading to succinate accumulation due to WI. To assess this we measured the core and the surface temperatures of a pig heart (~300 g) during flushing with cold preservation solution via the aortic root cannula immediately after cross clamp in conjunction with topical application of ice 'slush' (Fig. 4a), as occurs during human heart transplantation. The core took ~15 min to reach 4 ˚C, despite using the same rapid cooling procedures used during clinical heart transplantation. This slow cooling led to significant succinate accumulation (Fig. 4b). Therefore, the inevitable periods of WI during organ retrieval, cooling and storage during transplantation will lead to significant succinate accumulation.

Measuring mouse heart temperature during retrieval for transplantation indicated that after the blood supply was stopped, the organ cooled slowly while the vessels were being prepared for transplantation, despite frequent topical application of cold saline (Supplementary Fig. 6d). This period of ischaemia as the organ cooled led to succinate accumulation that was retained during subsequent cold storage (Supplementary Fig. 6e). To determine whether the accumulated succinate could contribute to tissue damage by driving IR injury upon reperfusion during transplantation, we used a mouse model of syngeneic transplantation, in which a heart is transplanted heterotopically into the abdomen[13,14]. During transplantation, there is a further period of ~20 min ischaemia as the heart is anastomosed to the blood vessels in the recipient mouse. During this time the heart gradually warmed up, despite cooling by topical saline, leading to a further accumulation of succinate (Fig. 4c). Within 5 min of reperfusion following transplantation the succinate level returned to baseline (Fig. 4c). Therefore during retrieval, storage and transplantation donor hearts accumulate succinate that is rapidly oxidised upon reperfusion in the recipient.

To model the slower cooling of a human heart during retrieval, we then assessed whether increasing the duration of WI (in addition to the ~8 min during retrieval and the ~20 min during anastomosis in the recipient) contributed to damage upon transplantation (Fig. 4d). Hearts did not survive transplantation when exposed to more than ~12 min WI after retrieval. Hearts transplanted after a further 12 min WI had increased damage evaluated 24 h after transplantation by release of troponin (Fig 4e) and mtDNA[15,16] (Figs. 4f,g) and by damage to mtDNA within the tissue (Fig. 4h). As the extra period of WI will increase succinate levels (Fig. 4c), these findings are consistent with increased WI contributing to heart damage through elevated succinate driving mitochondrial ROS production upon reperfusion. However, many other factors may contribute to tissue damage in addition to succinate. Therefore, we next explored the role of succinate accumulation alone in the absence of other confounding factors associated with WI.

To assess the role of succinate accumulation on heart damage upon transplantation independently of other effects of WI, we increased heart succinate levels by infusing *bis*-acetoxymethyl succinate (AMS)[17]. AMS generates succinate within cells that can then be oxidised by SDH[17]. Hearts were incubated at 37˚C for 20 min, to mimic the time taken for anastomosis of the heart in the recipient, followed by 30 min CI. Addition of AMS after CI greatly increased tissue succinate levels above that due to WI alone due to enhanced hydrolysis of AMS at 37˚C (Supplementary Fig. 6f). AMS-treated hearts exhibited increase damage upon transplantation, as measured 24 h later by the release of troponin (Fig. 4e) and mtDNA (Figs. 4f,g) and by damage to mtDNA within the transplanted heart (Fig. 4h). Infusion of the same amount of *bis*-acetoxymethyl fumarate, which readily delivers fumarate within cells (Supplementary Figs. 6g), did not lead to damage (Supplementary Figs. 6h,i), indicating that disruption to cardiac damage is specific to succinate over other TCA cycle intermediates. These findings show that succinate alone is sufficient to cause extensive damage to the transplanted heart. This is consistent with succinate accumulation being responsible for at least part of the increased heart damage caused by 12 min further WI.

Finally, to determine if this increased heart damage due to 12 min further WI was decreased by inhibiting succinate accumulation and oxidation, we infused dimethyl malonate (DMM) prior to initiating retrieval and cold storage to load the heart with

malonate (Fig. 4d, Supplementary Fig. 6j). Hydrolysis of DMM will generate the SDH inhibitor malonate within the tissues slowing both the accumulation of succinate during ischaemia (Supplementary Fig. 6k) and its oxidation upon reperfusion, thereby protecting against IR injury[4,18,19]. DMM protected the heart against damage measured 24 hours after transplantation (Figs. 4e-h). Thus, succinate accumulation during WI and its oxidation upon reperfusion is a significant contributor to IR injury in transplantation and its amelioration decreases organ injury.

We can draw a number of significant conclusions from our assessment of metabolic changes during WI and CI in mouse, pig, and human heart. Firstly, metabolism during WI and CI was comparable between mice, pigs and human hearts, encouraging the development of therapies using animal models. Secondly, during WI there was a dramatic decrease in the ATP/ADP ratio that is slowed by CI. The fall in ATP/ADP ratio during WI was paralleled by the generation of AMP via adenylate kinase, leading to AMP breakdown and an accumulation of purine and pyrimidine breakdown products. Therefore a major benefit of CI is preserving the ATP/ADP ratio and preventing loss of adenine nucleotides, the loss of which likely contributes to increased RET at reperfusion[20]. Thirdly, there was a rapid decrease in glycogen with WI and an associated increase in lactate, consistent with anaerobic glycolysis driving ATP production. This loss of glycogen and production of lactate was far faster in WI than CI, but interestingly there was incomplete breakdown of glycogen in WI, suggesting that the rising NADH/NAD^+ ratio and/or the falling ADP level slowed glycolysis and glycogenolysis. Finally, and most interestingly, succinate accumulated very rapidly in all species during WI. Ischaemic succinate accumulation most likely arises as a consequence of the build-up of NADH and other metabolites contributing to succinate generation by reversal of SDH[3,4]. However, further work will be required to assess whether glutaminolysis also contributes to succinate accumulation during WI, as recently proposed[21]. This selective accumulation of succinate over other TCA metabolites during ischaemia may be the consequence of multiple metabolic reactions that converge on succinate, which cannot be metabolised further under these conditions, in contrast to other TCA metabolites.

Importantly, succinate accumulation occurred when we simulated donation after brain stem death (DBD) in which normoxaemic organs are cooled *in situ* immediately

after cessation of circulation and are therefore often considered to be exposed to 'cold ischaemia' only. However, these organs are exposed to at least a few minutes of 'warm ischaemia' as the organs become ischaemic and cooling commences, but before the organ reaches ~2°C. Thus damage caused by WI is an inevitable, albeit not widely recognised, part of all transplantation despite the widespread reliance on cold flush and storage to enhance organ preservation.

In summary, in the first application of detailed and time-resolved metabolomics to transplant surgery we have shown that succinate accumulation is an important but underappreciated cause of pathology during organ transplantation. We propose that preventing the accumulation and oxidation of succinate during transplantation with new therapies and changes in methodology to ensure more rapid cooling will improve the outcome of transplantation.

References

1. Jahania, M. S., Sanchez, J. A., Narayan, P., Lasley, R. D. & Mentzer, R. M., Jr. Heart preservation for transplantation: principles and strategies. *Ann. Thorac. Surg.* **68**, 1983-1987 (1999).
2. Southard, J. H. & Belzer, F. O. Organ preservation. *Annu Rev Med* **46**, 235-247 (1995).
3. Chouchani, E. T. *et al.* A unifying mechanism for mitochondrial superoxide production during ischemia-reperfusion injury. *Cell Metab.* **23**, 254-263,(2016).
4. Chouchani, E. T. *et al.* Ischaemic accumulation of succinate controls reperfusion injury through mitochondrial ROS. *Nature* **515**, 431-435 (2014).
5. Pagani, F. D. Use of heart donors following circulatory death: A viable addition to the heart donor pool. *J. Am. Coll. Cardiol.* **73**, 1460-1462 (2019).
6. Johnson, R. J., Bradbury, L. L., Martin, K. & Neuberger, J. Organ donation and transplantation in the UK-the last decade: a report from the UK national transplant registry. *Transplantation* **97**, S1-S27 (2014).
7. Chew, H. C. *et al.* Outcomes of donation after circulatory death heart transplantation in australia. *J. Am. Coll. Cardiol*. **73**, 1447-1459 (2019).
8. Dhital, K. K. *et al.* Adult heart transplantation with distant procurement and ex-vivo preservation of donor hearts after circulatory death: a case series. *Lancet* **385**, 2585-2591 (2015).
9. Nasralla, D. *et al.* A randomized trial of normothermic preservation in liver transplantation. *Nature*, **557**, 50-56 (2018).
10. Coffey, J. C. *et al.* The influence of functional warm ischemia time on DCD liver transplant recipients' outcomes. *Clin. Transplant.* **31**, e13068 (2017).
11. Blok, J. J. *et al.* Longterm results of liver transplantation from donation after circulatory death. *Liver Transplant.* **22**, 1107-1114 (2016).

12. Eltzschig, H. K. & Eckle, T. Ischemia and reperfusion--from mechanism to translation. *Nat. Med.* **17**, 1391-1401 (2011).
13. Liu, F. & Kang, S. M. Heterotopic heart transplantation in mice. *J Vis. Exp.* **6**, 238 (2007).
14. Niimi, M. The technique for heterotopic cardiac transplantation in mice: experience of 3000 operations by one surgeon. *J. Heart Lung Transplant.* **20**, 1123-1128 (2001).
15. Zhang, Q. *et al.* Circulating mitochondrial DAMPs cause inflammatory responses to injury. *Nature* **464**, 104-107 (2010).
16. Nakahira, K. *et al.* Circulating mitochondrial DNA in patients in the ICU as a marker of mortality: derivation and validation. *PLoS Med.* **10**, e1001577 (2013).
17. Ehinger, J. K. *et al.* Cell-permeable succinate prodrugs bypass mitochondrial complex I deficiency. *Nat. Commun.* **7**, 12317 (2016).
18. Valls-Lacalle, L. *et al.* Selective Inhibition of succinate dehydrogenase in reperfused myocardium with intracoronary malonate reduces infarct size. *Sci. Rep.* **8**, 2442 (2018).
19. Valls-Lacalle, L. *et al.* Succinate dehydrogenase inhibition with malonate during reperfusion reduces infarct size by preventing mitochondrial permeability transition. *Cardiovasc. Res.* **109**, 374-384 (2016).
20. Bundgaard, A. *et al.* Metabolic adaptations during extreme anoxia in the turtle heart and their implications for ischemia-reperfusion injury. *Sci. Rep.* **9**, 2850, (2019).
21. Zhang, J. *et al.* Accumulation of succinate in cardiac ischemia primarily occurs via canonical krebs cycle activity. *Cell Rep.* **23**, 2617-2628 (2018).
22. Dare, A. J. *et al.* The mitochondria-targeted anti-oxidant MitoQ decreases ischemia-reperfusion injury in a murine syngeneic heart transplant model. *J. Heart Lung Transplant.* **34**, 1471-1480 (2015).
23. Mackay, G. M., Zheng, L., van den Broek, N. J. & Gottlieb, E. Analysis of cell metabolism using LC-MS and isotope tracers. *Meth. Enzymol.* **561**, 171-196 (2015).
24. Strehler, B. L. in *Methods in Enzymatic analysis* (ed U. Bergmeyer) 2112-2126 (Academic Press, 1974).
25. Passonneau, J. V. & Lauderdale, V. R. A comparison of three methods of glycogen measurement in tissues. *Anal. Biochem.* **60**, 405-412 (1974).
26. Santos, J. H., Meyer, J. N., Mandavilli, B. S. & Van Houten, B. Quantitative PCR-based measurement of nuclear and mitochondrial DNA damage and repair in mammalian cells. *Methods Mol. Biol.* **314**, 183-199 (2006).
27. Ritchie, M. E., Phipson, B., Wu, D., Hu, Y., Law, C. W., Shi, W., & Smyth, G.K. Limma powers differential expression analyses for RNA-sequencing and microarray studies. *Nuc Acids Res.* **43**, e47 (2015).

Methods

Materials. The composition of UW storage solution used is (mM): potassium lactobionate, 50; KH_2PO_4, 25; $MgSO_4$, 5; raffinose, 30; adenosine, 5; glutathione, 3; allopurinol, 1; and hydroxyethyl starch (50 g/L). The composition of St Thomas's cardioplegia solution is: (NaCl 110.0 mM, $NaHCO_3$ 10.0 mM, KCl 16.0 mM, $MgCl_2$ 16.0 mM, $CaCl_2$ 1.2 mM, pH 7.8). Dimethyl malonate was from Thermo Fisher Scientific, UK. Tissue samples were incubated in polypropylene tubes, either 1.5 ml (Ref:72.690.001) or 50 mL (Ref: 62.547.004), both from Sarstedt, Nümbrecht, Germany.

Animals. Female mice (C57BL/6J (B6/J) **)** of 10 – 20 weeks of age, weighing 16-22g were purchased from Charles River Laboratories, UK. Mice were maintained in specific-pathogen-free animal facilities with *ad libitum* access to food and water. Mice were picked at random from the same cage and assigned to control and experimental arms, but no effort was made to ensure that littermate controls. Large white male (Landrace) pigs (45-55 kg) were supplied by Envigo and were acclimatised for a minimum of 7 days prior to experiments, with *ad libitum* access to food and water. All animal experiments were approved by the UK Home Office under the Animals (Scientific Procedures) Act 1986. Mouse experiments were covered by PPL 80/2638.

Human tissue. Heart biopsies were taken from deceased human DBD donors deemed unsuitable for cardiac transplantation aged 36-69 (Table S1). Informed consent for the use of the human tissue for this project was provided by the donors' families. Ethical approval for the studies was obtained from NRES Committee East of England – Cambridge South (REC Reference 15/EE/0152).

Mouse heart experiments. C57BL/6 mice (female) were anaesthetised with isoflurane (Abbott Laboratories, US) 2 MAC and O_2 at 2 L/min. Heparin (100 µL bolus (25 iU) Leo Pharma A/S, Ballerup, Denmark) was administered intravenously into the inferior vena cava (IVC) prior to retrieval. Hearts were excised by division of the major vessels. To

measure metabolite concentrations in the heart under baseline conditions *in vivo*, the still-beating heart of an anesthetised mouse was rapidly frozen using Wollenberg clamps at liquid nitrogen (LN_2) temperature, taking $\leq$ 5 s to go from the beating heart to frozen. For cold ischemia (CI) the heart was placed directly in UW solution at ~2°C. Under these conditions the ventricles pulsed once or twice before stopping. For warm ischaemia (WI) the excised heart was left in the abdomen of the animal, with the abdominal wound closed and the animal maintained on a 37°C heating pad with a relayed rectal temperature probe. For analysis at various times the whole heart was clamped at LN_2 temperature as above. At various times the tissues were rapidly snap-frozen and stored at -80˚C until analysis. Fully oxygenated 'normoxic' heart tissue, snap-frozen immediately upon cessation of circulation, was used as control. Tissues were stored at -80°C until extraction and analysis.

To replicate heart retrieval with retrograde flushing of the coronary vessels during retrieval (Supplementary Fig. 4e) the donor animal was prepared as described above. Following exsanguination, the great vessels were prepared for implantation[22]. The thoracic cavity was entered by dividing the diaphragm and adequate exposure achieved by dividing the ribs laterally up to the thoracic inlet and retracting the anterior rib cage cranially. The IVC or caudal caval vein, left SVC or cranial caval vein and right SVC or cranial caval vein were ligated with silk ties. The fat and connective tissue was dissected between the aorta and pulmonary artery prior to division of the ascending aorta at the level of the innominate artery. If the heart were to be flushed, the innominate, right carotid and right brachiocephalic artery were ligated and divided. The descending aorta was then divided. The left and right pulmonary arteries were divided adjacent to their bifurcation and the connecting vessel wall divided to create a single opening. During dissection and ligation of vessels the heart was topically cooled intermittently with 0.9% w/v sodium chloride kept on ice. Following ligation of the pulmonary artery blood remaining in the ventricles was manually expressed. The pulmonary veins were ligated *en masse* and the heart excised. 500 µL Soltran® (Baxter Healthcare) was then injected via a fine bore (0.28 x 0.165 mm) polyethene tube (Portex tubing, Smith Medical International Ltd, UK) into the aorta to antegrade flush the coronary arteries. The prepared hearts were then placed in UW solution at ~2°C for various durations of CI after which, the whole

heart was clamped at LN_2 temperature as above. For other mouse heart experiments, a 500 µL bolus of St Thomas' Cardioplegia solution was administered by IVC injection. Complete cessation of a heart beat was observed visually within 2 seconds. Dimethyl malonate (DMM) was administered as an infusion over 10 minutes via the IVC by a microinfusion pump (Kd Scientific, Holliston, MA, USA) using a fine bore (0.28 x 0.165 mm) polyethene tube (Portex tubing, Smith Medical International Ltd, UK) prior to the administration of cardioplegia. Control animals were infused with 0.9% w/v sodium chloride by microinfusion pump (Kd Scientific, Holliston, MA, USA). Bis(acetoxymethyl)succinate (with 5% DMSO) or bis(acetoxymethyl)fumarate (with 30% DMSO) was administered in the cardioplegia solution. Hearts from donor mice were transplanted heterotopically into a syngeneic recipient[13,14]. The donor heart was transplanted heterotopically into the abdomen of the recipient animal using a microsurgical technique. The recipient mouse was weighed before being anaesthetised with isoflurane (Abbott Laboratories, US) and oxygen at 2 l/min. The skin at the operative site was shaved and prepped with chlorhexidine gluconate (4% w/v). Analgesia was administered by subcutaneous injection of 100 µl Temgesic (Indivior, UK) diluted in 500 µl 0.9% w/v sodium chloride to the nape of the animal. The animal was transferred to the operating table, secured in a supine position using adhesive tape and the animal's rectal temperature was measured continuously using a rectal thermometer and maintained at 37°C ± 1°C using a relayed variable heat mat. A midline laparotomy was performed and the abdominal and exposure achieved using a self-retaining retractor. The urinary bladder was emptied by gentle pressure using sterile cotton buds. The small bowel and colon were deflected superiorly and a small strip of connective tissue divided to facilitate this manoeuvre. The abdominal viscera were retracted and covered with moistened sterile gauze to provide adequate exposure to the abdominal aorta and IVC and adequate moisture maintained throughout the procedure by periodic topical irrigation. The connective tissue overlying the abdominal aorta and IVC was divided by a combination of sharp and blunt dissection. The posterior lumbar vessels were identified and ligated using 7-0 silk ties. Non-crushing vascular clamps were applied to the vessels distal to the renal vessels and proximal to their bifurcation. The IVC was emptied via a venotomy created with a 31-gauge needle. An arteriotomy was then made in the aorta and this was

extended using micro-surgical scissors to match the diameter of the donor aorta. The lumen was flushed with 0.9% w/v sodium chloride to remove any remaining blood and clots. The donor heart was then retrieved from cold storage and placed into the right side of the recipient's abdomen with the remnant ascending aorta adjacent to the arteriotomy. A small piece of gauze moistened with cold (1-2°C) 0.9% w/v sodium chloride was placed over the heart to minimise warming and periodic topical application of (1-2°C) 0.9% w/v sodium chloride was applied to the donor heart during the procedure. Cranial and caudal stay sutures were placed between the donor and recipient vessels using 10-0 nylon Bear™ surgical suture on a round bodied 4 mm (3/8) needle (Bear Medic Corp., Tokyo, Japan). A continuous end-to-side anastomosis run in a counter clockwise direction was then constructed from the caudal stay suture. After completing one side of the anastomosis, the heart was turned to the animal's left side to enable access and completion of the anastomosis. The venotomy on the IVC was then extended in a cranial direction. The pulmonary artery was anastomosed in a similar fashion using 10-0 nylon Bear™ surgical suture. Over tightening of sutures was minimised to ensure there was no constriction of the anastomosis. Cut pieces of Surgicel (Ethicon, Johnson and Johnson, US) were applied around the anastomosis. The distal clamp was removed followed by the proximal clamp. Satisfactory perfusion was indicated by a bright red heart displaying strong rhythmic contractions and warmed topical 0.9% w/v sodium chloride was applied to the heart to expedite this process. The abdominal fascia and skin were closed in two layers with continuous 5-0 vicryl™ (Ethicon, Johnson and Johnson, UK). Following reperfusion and closure of the midline wound 500 µl of 0.9% sterile saline was injected subcutaneously. Animals were recovered in an incubator at 28°C overnight on soft, dry bedding with food and water. Animals that developed post-operative hind limb paralysis were killed immediately. The next day animals were returned to standard cages with standard rodent diets. All transplanted hearts contracted spontaneously following reperfusion. Hearts were excised by division of the anastomosed vessels at chosen time points after reperfusion and the hearts were snap frozen using a Wollenberg clamp and stored at -80°C until tissue extraction. Animals were randomly allocated to control and treatment groups and the analysis performed blinded to the experimental groups.

Pig heart experiments. Pigs were pre-medicated with intramuscular ketamine (10 $mg.kg^{-1}$), medetomidine (0.02 $mg.kg^{-1}$) and midazolam (0.1 $mg.kg^{-1}$). A peripheral intravenous catheter was placed in the marginal ear vein and anaesthesia was induced with propofol. Pigs were intubated and 100% oxygen supplied with intermittent positive pressure ventilation provided to maintain normocapnia. Anaesthesia was maintained with continuous infusions of propofol (starting at 10 $mg.kg^{-1}hr^{-1}$ and titrating down to effect) and either remifentanil (starting at 2.4 $\mu g.kg^{-1}hr^{-1}$ and titrating up to effect) or alfentanil (starting at 30 $\mu g.kg^{-1}hr^{-1}$ and titrating up to effect). If required, isoflurane was provided at approximately 2% to maintain anaesthesia. Saline was administered intravenously at approximately 10 $ml.kg^{-1}hr^{-1}$. During anaesthesia a Datex Ohmeda Cardiocap patient monitoring system was used to monitor ECG waveform, pulse oximetry, temperature and capnography parameters. Immediately following euthanisation (induced rapidly with an overdose of approximately 200 $mg.kg^{-1}$ pentobarbitone) the thoracic cavity was accessed through the diaphragm and the apex of the heart (~20-30 g) was amputated with a scalpel under terminal anaesthesia. We note that this retrieval procedure, particularly the use of anaesthesia is unavoidable, but is slightly different from that used in human transplantation. A full thickness tissue sample (~120 mg) was immediately clamped frozen using Wollenberger clamps at LN_2 temperature, taking $\leq$ 5 s from cessation of aortic pulse to freezing. The rest of the tissue was cut in half with one half transferred to cold storage solution and then further cut into smaller pieces (~120 mg) which were then stored in UW storage solution at ~2˚C. The other half of the heart tissue was also cut into sections (~120 mg) which were stored in a humidified atmosphere at 37˚C by suspension above saline in sealed Eppendorf tubes. At various times the tissues were then frozen using Wollenberger clamps at LN_2 temperature and stored at -80˚C until analysis.

To measure the core and surface temperature and tissue succinate of the porcine heart following rapid retrieval and back-table flush the pig was anaesthetised and euthanized as described above. After circulatory arrest was confirmed the thoracic cavity was then rapidly accessed through an incision in the diaphragm and heart was rapidly retrieved by division of the great vessels. On removal from the thoracic cavity, a ‘time-zero’ surface wedge and core needle biopsy were immediately taken and clamp frozen in liquid nitrogen. The core and surface temperature probes (K-type thermocouple, Hanna

Instruments, Bedfordshire) were then inserted into the heart. The core temperature probe was inserted into the septum using a hollow biopsy needle. A small incision was made in the surface of the right ventricle in which the surface probe was inserted and sutured in place. This step took between 1-2 minutes to complete. Temperature recording was then commenced and the heart was submerged in a pre-prepared dish of slushed ice and UW solution. The temperature was recorded every second by a digital data-logger connected to the temperature probe (EL-USB-2 LC, Lascar Electronics, Wiltshire). A 14G French cannula was used to flush the coronary circulation with cold UW solution. A third temperature probe was used to measure the temperature of the solution as it entered the heart. The coronary sinuses at the base of the aorta were alternately cannulated and effective flushing of the circulation could be directly observed by flushing of blood with preservation solution in the surface coronary vessels. The time taken to flush the heart with 500 mL cold UW solution was recorded in each case. Further surface wedge and core-needle biopsies were taken at 6, 12 and 30 minutes.

Human heart experiments. Human donation after brainstem death (DBD) donors undergoing abdominal multi-organ retrieval but for whom cardiothoracic organs had been declined for transplantation were identified (Supplementary Table 1). Appropriate consent for research was obtained from the donor families. A thoracotomy was performed as a routine part of the abdominal organ retrieval procedure, thus allowing a sample (~20-30 g) of myocardium from the apex of the still-beating heart to be removed at the same time as exsanguination and cross clamp of the donor, during organ retrieval. The heart tissue was frozen in Wollenberg clamps, taking <5s to go from the beating oxygenated heart to frozen sample. After this base line sample, further samples (~120 mg) were removed, maintained at either 37˚C or ~2˚C as described for the pig tissue, and at various times frozen and stored at -80˚C.

Tissue extraction and metabolite analysis by liquid chromatography coupled to mass spectrometry (LC-MS). Frozen tissue samples were weighed into Precellys tubes prefilled with ceramic beads (Stretton Scientific Ltd., Derbyshire, UK), and an exact volume of extraction solution (50% methanol, 30% acetonitrile and 20% water) was

added to obtain 40 mg specimen per mL of extraction solution thus allowing for comparisons between experimental conditions for the same metabolite. Samples were lysed using a Precellys®24 tissue homogeniser (Bertin Corp, Rockville, MD 20850, USA. 5500 rpm 15 seconds x 2) and then centrifuged (16,162 x g for 10 min at 4°C). The supernatant was transferred to glass vials (Microsolv Technology Corp., Leland, NC 28451, USA) and stored at -80°C until LC-MS analysis.

LC-MS analyses were performed on a Q Exactive Orbitrap (Thermo Scientific) mass spectrometer coupled to an Ultimate 3000 RSLC system (Dionex). The liquid chromatography system was fitted with either a ZIC-HILIC column (150 mm × 4.6 mm) or a ZIC-pHILIC column (150 mm × 2.1 mm) and respective guard columns (20 mm × 2.1 mm) (all Merck, Germany)[23]. For the ZIC-HILIC column the flow rate was 300 µl/min and the gradient comprised 0.1% formic acid/water and 0.1% formic acid /acetonitrile as follows (time (min), % acetonitrile): 0, 80; 12, 50; 26, 50; 28, 20; 36, 20; 37, 80;45, 80. For the ZIC-pHILIC column the flow rate was 200 µl/min and the gradient comprised 20 mM $(NH_4)_2CO_3$, pH 9.4 and acetonitrile as follows (time (min), % acetonitrile): 0, 80; 2, 80; 17, 20; 17.1, 80; 19.1, 80; 22.1, 80;22.2, 80, with an increase in flow rate to 400 µl/min from 19.1 to 22.1. The mass spectrometer was operated in full MS and polarity switching mode. Samples were randomised in order to avoid bias due to machine drift and processed blindly. The acquired spectra were analysed using XCalibur Qual and and XCalibur Quan Browser software (Thermo Fisher Scientific) by referencing to an internal library of compounds. Absolute quantification of selected metabolites was performed by interpolation of the corresponding standard curve obtained from serial dilutions of commercially available standards (Sigma Aldrich) running with the same batch of samples. All the extractions and analyses were done under the same conditions and relative to the same internal standard. The NADH/NAD^+, lactate/pyruvate and succinate/fumarate ratios are presented as relative changes in the ratio of the ion current for these metabolites, which is proportional to, but not the same as, the true ratio of the metabolite levels.

LC-MS/MS analysis of succinate and malonate from pig, mouse and human temperature studies and fumarate delivery from *bis*-acetoxymethyl fumarate in cells was performed using an LCMS-8060 mass spectrometer (Shimadzu, UK) with a Nexera X2

519 UHPLC system (Shimadzu, UK). Samples were stored in a refrigerated autosampler (4
520 °C) upon injection of 5 µl into a 15 µl flow through needle. Separation was achieved
521 using a SeQuant® ZIC®-HILIC column (3.5 µm, 100 Å, 150 x 2.1 mm, 30 °C column
522 temperature; MerckMillipore, UK) with a ZIC®-HILIC guard column (200 Å, 1 x 5mm).
523 A flow rate of 200 µl/min was used with mobile phases of A) 100 mM ammonium
524 acetate (pH 6.9) and B) 100% acetonitrile. A gradient of 0-0.1 min, 80% MS buffer B;
525 0.1-4 min, 80%-20% B; 4-10 min, 20% B, 10-11 min, 20%-80% B; 11-15 min, 80% B
526 was used. The mass spectrometer was operated in negative ion mode with multiple
527 reaction monitoring (MRM) and spectra were acquired using Labsolutions software
528 (Shimadzu, UK), with compound quantities calculated from relevant standard curves
529 (succinate, malonate or fumarate) in MS extraction buffer and comparing against ^{13}C-
530 succinate (for succinate and fumarate) or ^{13}C-malonate (for malonate) internal standards.
531 Metabolomic data have been uploaded as study MTBLS1085 to MetaboLights
532 (https://www.ebi.ac.uk/metabolights).
533
534 **Tissue analysis for ATP/ADP ratio.** ATP and ADP concentrations were measured using
535 a Luciferase based assay [24]. Frozen tissue samples were homogenised in ice-cold
536 perchloric acid extractant (3% v/v $HClO_4$, 2 mM Na_2EDTA, 0.5% Triton X-100). The
537 supernatant was diluted to a concentration of 1 mg frozen tissue /ml. Samples, ATP and
538 ADP standards were pH neutralized using a potassium hydroxide solution (2 M KOH,
539 2 mM Na_2EDTA, 50 mM MOPS), vortexed until formation of a white precipitate
540 ($KClO_4$), then centrifuged (17, 000 X g for 1 min at 4°C). For ADP measurements, 250
541 µl neutralised sample supernatant was mixed with 250 µl ATP sulfurylase assay buffer
542 (20 mM Na_2MoO_4, 5 mM GMP, 0.2 U ATP sulfurylase (New England Biolabs), in Tris-
543 HCl buffer (100 mM Tris-HCl, 10 mM $MgCl_2$ (pH 8.0))), incubated for 30 min at 30^{O}C
544 with shaking (500 rpm), heated at 100˚C for 5 min and then cooled on ice. Standards (100
545 µl), samples for ATP measurement (100 µl) or samples for ADP measurement (200 µl)
546 (in duplicate) were added to 400 µl Tris-acetate (TA) buffer (100 mM Tris, 2 mM
547 Na_2EDTA, 50 mM $MgCl_2$, pH 7.75 with glacial acetic acid) in luminometer tubes. 10 µl
548 pyruvate kinase solution (100 mM PEP, 6 U pyruvate kinase suspension (Sigma #
549 P1506)) were added to one set of samples for ADP measurement and incubated for 30

min at 25°C in the dark to convert ADP to ATP. The other duplicate tube (without addition of pyruvate kinase solution) served as an ADP 'blank' value. The samples were then all assayed for ATP content in a Berthold AutoLumat Plus luminometer by addition of 100 µl Luciferase/Luciferin Solution (7.5 mM DTT, 0.4 mg/ml BSA, 1.92 µg luciferase/ml (SIGMA #L9506), 120 µM D-luciferin (SIGMA # L9504), made in TA buffer (25% v/v glycerol)), delivered via auto injection, protected from light. Bioluminescence of the ATP-dependent luciferase activity was measured for 45 s post injection and the data quantified against standard curves.

Glycogen assay. The glycogen assay protocol was adapted from[25], measuring the production of NA(D)PH during the oxidation of glycogen-derived glucose to 6-phosphogluconate. Frozen tissue (5-10 mg) was minced finely before being treated with 250 µl hot acid (2 M HCl; 100°C) or alkali (2 M NaOH; 100°C) to hydrolyse glycogen or as an unhydrolysed control respectively (100 °C, 1 h, vigorous shaking every 10 min). Samples were subsequently cooled to RT and neutralised to pH 7 with either 2 M NaOH or HCl and the addition of 500 µl 400 mM Tris (pH 7.4). Neutralised samples were vortexed before centrifuging (17,000 x g, 10 min, RT). 60 µl of sample supernatant was plated in duplicate in a 96-well plate together with a glucose standard curve (0,10, 20, 40, 80, 160 µg glucose/ml). 200 µl glucose assay reagent (G3293, Sigma) was added to each well and the plate incubated (5 min, RT) prior to measuring absorbance at 340 nm in a Spectramax Plus 384 plate reader (Molecular Devices, UK). The average absorbance of each sample was interpolated using the standard curve and multiplied by the final volume after pH adjustment to give µg of glycogen (or glucose for NaOH control) in original sample. This was divided by the weight of tissue added and the NaOH control was subtracted from the HCl sample to give µg glycogen per mg frozen tissue.

Synthesis of bis(acetoxymethyl)succinate. Bis(acetoxymethyl)succinate (202 mg, 0.769 mmol) was prepared in 91% yield from succinic acid (100 mg, 0.847 mmol) in a similar way to Ehinger et al.,[17] except acetonitrile was used as solvent and after 16 h reaction the solvent was evaporated and the crude mixture purified by column chromatography [SiO_2, hexane-ethyl acetate (7:3)]. R_f [SiO_2, hexane-ethyl acetate (7:3)] = 0.24. ν_{max} (ATR):

1751 (CO) cm^{-1}. δ_H (400 MHz, $CDCl_3$): 5.75 (4H, s, OCH_2O), 2.71 (4H, s, CH_2CO_2), 2.12 (6H, s, CH_3). δ_C (126 MHz, $CDCl_3$): 170.93 (2C, s, CO), 169.71 (2C, s, CO), 79.38 (2C, s, CH_2O), 28.66 (2C, s, **C**H_2CO), 20.80 (2C, s, CH_3). LRMS (ESI^+): 285 (MNa^+, 100%). HRMS (ESI^+): 285.0579. $C_{10}H_{14}NaO_8^+$ requires (MNa^+), 285.0581. ^1H NMR and ^{13}C NMR data agree with literature[17]. See Supplementary Fig. 7. The original data has been deposited at http://dx.doi.org/10.5525/gla.researchdata.646.

Synthesis of bis(acetoxymethyl) fumarate. Bromomethyl acetate (300 µl, 3.06 mmol, 2.2 eq) was added to a solution of fumaric acid (161 mg, 1.39 mmol, 1.0 eq) and diisopropylamine (605 µl, 3.47 mmol, 2.5 eq) in dry acetonitrile (8 ml) cooled to 0 °C under argon. The solution was allowed to warm to room temperature, stirred overnight, concentrated under vacuum and purified by column chromatography [SiO_2, hexane-ethyl acetate (80:20) to (50:50)] to give the bis-AM ester as a white solid (310 mg, 86%). R_f [SiO_2, hexane-ethyl acetate (7:3)] = 0.31. M.p. 89-91°C. ν_{max} (ATR)/cm^{-1}: 1755 (CO_2), 1728 (CO_2), 977 (C=C). δ_H (400 MHz: $CDCl_3$): 2.12 (6H, s, CH_3), 5.84 (CH_2), 6.92 (CH). δ_C (100 MHz: $CDCl_3$): 20.76 (CH_3), 79.80 (CH_2), 133.98 (CH), 163.27 (C), 169.51 (C). HRMS (ESI^+): 283.0423. $C_{10}H_{12}NaO_8$ requires (MNa^+), 283.0424. See Supplementary Fig. 7. The original data have been deposited at http://dx.doi.org/10.5525/gla.researchdata.646.

Troponin measurement. Non-heparinised IVC blood samples were taken immediately prior to graft harvest. Samples were left for 30 mins at room temperature to ensure adequate clot propagation, centrifuged (2000 x g for 10 minutes) and serum apportioned into aliquots and stored at -80°C. Serum troponin-I was measured using a commercially available mouse cardiac troponin-I ELISA (KT-470, Kamiya Biomedical Company, Seattle, WA, USA) by the Core Biomedical Analysis Laboratory, Addenbrooke's Hospital, Cambridge.

Measurement of mtDNA release. The release of mitochondrial and nuclear DNA into the circulation was assessed using the droplet digital polymerase chain reaction (ddPCR). Serum samples were centrifuged (1600 g for 10 min) and the supernatant was then

612 centrifuged once more (16 000 g for 10 min) and DNA isolated using the DNeasy Blood
613 kit (QIAGEN) according to the manufacturer's instructions, with step 3, the addition of
614 lysis buffer AL, omitted. DNA was quantified using a 'Nanodrop' system and diluted to 1
615 ng/μL in elution buffer. For mtDNA the ND5 gene was assessed using the following
616 primers: F- CTGCTCTTTCCCAGACGAGG; R- AAGGCCACTTATCACCAGC. For
617 nuclear DNA the β-actin gene was assessed, using F-
618 ACCTAATTAAACACATCAACTTCCC; R- GACTCAGTGCCAGGTTGTAA. Each
619 PCR reaction (22 μL) comprised 1 μL (= 1 ng) DNA template, 11 μL ddPCR
620 Supermix (no dUTP) containing Taq, 314 nM of each primer, and 210 nM of the HEX-
621 ND5 probe (ACACCACCACATCAATCAAATTCTCCTTCA) and of the FAM-β-actin
622 probe (ATTGCCTTTCTGACTAGGTG) and then made up to 22 μl with H_2O. The
623 BIORAD ddPCR AutoDG was used to generate ddPCR droplets and the plate was sealed
624 at 174˚C before the PCR was run in a BIORAD C1000 Thermo Cycler: 95˚C at 10 min
625 followed by 40 cycles of 30 sec at 95˚C and 1 min at 58˚C and then 95˚C at 10 min. After
626 completion of the PCR, the fluorescence of the FAM and HEX probes was measured
627 using the BIORAD QX200 Droplet Reader and analysed using the BIORAD Quantilife
628 software and Excel.
629
630 **QPCR assay for mtDNA damage.** Quantitative PCR to detect murine mitochondrial
631 DNA lesions was based on[26] and performed using following primers at 10 μM: forward
632 primer FWD: 5'-GCC AGC CTG ACC CAT AGC CAT AAT-3'. Reverse primer for the
633 long 10090 bp PCR product: REV: 5'-GAG AGA TTT TAT GGG TGT AAT GCG G-3'.
634 Reverse primer for the short 127 bp PCR product: REV: 5'- GCC GGC TGC GTA TTC
635 TAC GTT A -3'. Sample DNA was extracted using the QIAmp blood and tissue kit
636 following the provided instructions. QPCR was performed on 15 ng DNA in 35 μl
637 reactions on a PCR thermocycler (Biometra). 1 U TaKaRa LA Taq was used per reaction.
638 PCR master mix was prepared following the TaKaRa LA Taq instructions. Linearity of
639 the PCR reaction was confirmed for each sample by running a 1:2 diluted sample
640 simultaneously. Cycling parameters for the short reaction were 94ºC for 5 minutes
641 followed by 16 cycles of 94ºC for 30s, 64ºC for 45s, 72ºC for 45s, followed by 72ºC for
642 10 minutes. Conditions for the long amplification were 94ºC for 5 minutes followed by

18 cycles of 94ºC for 15s and 64ºC for 12 minutes, followed by 72ºC for 10 minutes. The PCR reaction was confirmed on 1% agarose gels and concentrations of the PCR product were determined by measuring the emission of the samples at 488 nm and excitation at 525 nm after picogreen addition at 1:200 dilution.

Cell culture. C2C12 mouse myoblast cells were plated at 300,000 cells/well in 6-well plates and left to adhere overnight. The following day, cells were treated with 0 (DMSO vehicle control), 0.25, 0.5 or 1 mM fumarate-AM diester for 30 min at 37 °C. Cells were washed 4 times with ice-cold PBS prior to extracting with 500 µl extraction buffer containing ^{13}C-succinate internal standard for 15 min on dry ice. Cells were scraped and transferred to microcentrifuge tubes prior to agitating (15 min, 4 °C, 1000 rpm), then incubating (-20 °C, 1 h). Samples were centrifuged (17,000 x g, 10 min, 4 °C), the supernatant transferred to fresh microcentrifuge tubes and recentrifuged (17,000 x g, 10 min, 4 °C). The resulting supernatant was transferred to glass MS vials and stored at -80 °C until analysis by LC-MS/MS. Fumarate levels were determined by interpolation of a fumarate standard curve and normalised to cellular protein by BCA assay of a parallel treated plate.

Statistics and experimental design. All data in figures are presented as mean values ± SEM unless otherwise stated. Statistical analysis was performed between two groups using Student's t-test with sometimes using Sidak's post-test for multiple comparisons, and between multiple groups by one-way analysis of variance (ANOVA) or two-way ANOVA with Bonferroni's or Tukey's multiple comparison testing. A P value of less than 0.05 was considered significant. For Fig 2, fold changes in metabolite abundances (and their statistical significance) between time points were calculated by using linear modelling with an empirical Bayes approach as implemented in the 'limma' package of R (ref 27). Regularised logs were taken of the abundance measurements of each metabolite, then the targets and the design matrix were defined for groups of samples to be compared, and the data fitted to a linear model. Contrasts were defined and significantly affected metabolites were identified from the fitted model by using their p-values, adjusting for multiple-testing by using the Benjamini0Hochberg procedure. Volcano plots

were produced by plotting the fold-change of each metabolite versus its adjusted p-value in R.

Data availability. Metabolomic data have been uploaded as study MTBLS1085 to MetaboLights (https://www.ebi.ac.uk/metabolights). The original synthetic chemistry data have been deposited at http://dx.doi.org/10.5525/gla.researchdata.646. Other data that support the findings of this study are available

Reporting Summary. Further information on research design is available in the Nature Research Reporting Summary linked to this article.

Acknowledgements

Work in the MPM laboratory was supported by the Medical Research Council UK (MC_U105663142) and by a Wellcome Trust Investigator award (110159/Z/15/Z) to MPM. Work in the CF laboratory was supported by the Medical Research Council (MRC_MC_UU_12022/6). Work in the KSP laboratory was supported by the Medical Research Council UK. Work in the RCH lab laboratory was supported by a Wellcome Trust Investigator award (110158/Z/15/Z) and a PhD studentship for LP from the University of Glasgow. AVG was supported by a PhD studentship funded by the National Institute for Health Research Blood and Transplant Research Unit (NIHR BTRU) in Organ Donation and Transplantation at the University of Cambridge in collaboration with Newcastle University and in partnership with NHS Blood and Transplant (NHSBT). The views expressed are those of the author(s) and not necessarily those of the NHS, the NIHR, the Department of Health or NHSBT. We are grateful to the donors, the donor families, National Health Service Blood transfusion and Transplantation, and the Cambridge Biorepository for Translational Medicine for access to human samples.

Author contributions

J.L.M., A.S.H.C., K.S.-P., R.C.H., T. K., M. H., K. M., C.F. and M.P.M. designed the experimental protocols. A.V.G., F.A., H.A.P., S.T.C., M.H., E.C.H., A.S.H.C., T.B., L.P., A. L., E. N. and J.L.M. performed the studies. J.L.M., A.S.H.C., A.M.J. and A. R.

analysed the data. J.L.M., A.S.H.C., K.S.-P., C.F., and M.P.M. wrote the manuscript with assistance from all the other authors.

Competing interests

The authors declare competing interests.

Figure legends

Fig. 1 | The cardiac ATP/ADP ratio during WI and CI a, A schematic illustrating the experimental design mimicking ischaemia during transplantation. The whole mouse heart (~150 – 180 mg), or sections from the transected apex of the pig or human heart (~120 mg) were either immediately clamped frozen at liquid nitrogen temperature to generate a baseline sample under fully oxygenated "normoxic" conditions, or incubated to induce warm ischaemia (WI, 37°C) or cold ischaemia (CI) (~2°C) for the indicated times prior to freeze clamping. Tissues were then extracted and metabolites assayed ATP and ADP were determined in heart tissue after various times of WI or CI. **b-d**, The ATP/ADP ratio for **b** mouse, **c** pig and **d** human. **e-g**, The sum of ATP and ADP (nmol/mg wet weight) for **e** mouse, **f** pig and **g** human. Data are means ± SEM, N = 5 (pig), 4 (human). For **b** and **e** data are means ± SEM, WI 6 and CI 240 min, N = 11; WI 0, 12, 30 and CI 0 min, N = 9; CI 6 min, N = 7; CI 12 min, N = 4; CI 30 min, N = 3.

Fig. 2 | Volcano plots of metabolites that change significantly between 30 min WI and CI. Volcano plots showing $-\log_{10}$ of the adjusted p value plotted against the Log_2 of the fold-change in metabolite abundance between 30 min WI and 30 min CI for **a** mouse (N = 5), **b** pig (n = 5) and **c** human (N = 4). Fold-changes and p-values between time points were calculated by using linear modelling with an empirical Bayes approach as implemented in the 'limma' package of R, adjusting for multiple-testing by using the Benjamini-Hochberg procedure. Metabolites that changed in the same way in all three species are in red. Metabolites that changed in the same way in two of the species but were not detected, or did not change markedly, in the third are in green. Proprionylcarnitine, propcarn; acetyl carnitine, acetylcarn; succinyl adenosine, succaden; 3-hydroxybutyrate, 3HB; pyroglutamic acid, pyroglu; cysteine, cys.

Fig. 3 | Succinate levels in the heart during WI and CI. a-d, Fold change in succinate abundance under WI or CI, relative to normoxic heart tissue in **a, d** mouse (n = 6), **b** pig (n = 4) **c** human (n = 4). Data are means ± SEM. For **a-c** significant difference between groups were measured by two way ANOVA with multiple comparisons at individual

740 points by Sidak test (* P < 0.05, ** P < 0.01 *** P < 0.001, **** P < 0.0001). **e**,
741 Absolute succinate concentrations as described in **a** – **d.** Data are means ± SEM. Mouse
742 (n = 6), pig (n = 4) human (n = 4). **f-h**, Relative change in succinate/fumarate ratio under
743 WI or CI, compared to normoxic heart tissue. Data are means ± SEM. Mouse (n = 6), pig
744 (n = 4) human (n = 4). These data are presented as relative changes in the ratio of the ion
745 current for these metabolites, which is proportional to, but not the same as, the true ratio
746 of the metabolite levels.

747 **Fig. 4 | Preventing pathological consequences of succinate metabolism during heart**
748 **transplantation. a,** Surface and core temperature of pig heart during flush with cold UW
749 solution. Following retrieval the heart was flushed with cold solution and immersed in
750 slushed ice. The mean temperature (n = 4) every 10 s is shown ± SEM (shaded). The
751 inset shows the temperature probes. **b,** Surface and core succinate of the pig heart treated
752 as in **a**. Core and surface tissue biopsies were taken at 0, 6, 12 and 30 minutes, frozen and
753 succinate concentration measured (n = 3, Data are means ± SEM). *P < 0.05, by a two-
754 way ANOVA with Sidak's multiple comparison test. **c**, Succinate concentration in the
755 mouse heart after standard retrieval and 30 min CIT ('Isch.'), after standard retrieval and
756 30 min CIT and anastomosis ('Isch. + Impl.'), and finally after 5 min reperfusion
757 ('Reper.'). Data mean ± SEM (Cont and Isch + Impl, n = 6; Isch, n = 4; Reper, n = 3).
758 Compared to control (Cont.) by one-way ANOVA with Bonferroni multiple comparisons
759 tests (***P < 0.001, ****P < 0.0001). **d,** Schematic of heterotopic heart transplantation in
760 mice, with a further 12 min WI after retrieval, followed by 30 min cold storage. **e-g**,
761 Hearts were infused with DMM (3.4 mg) or saline prior to cardioplegia and then exposed
762 to 12 min WI, and then stored cold for 30 min, or infused with cardioplegia solution ±
763 AMS (3.2 mg), followed by cold storage for 30 min. All hearts were then transplanted
764 into recipients and 24 h later serum troponin **e**, mtDNA **f,** or mtDNA/nDNA ratio **g**, were
765 measured. **h**, mtDNA damage in the donor heart was measured 24 h after transplantation
766 by a PCR assay in which the greater the ratio of amplification the less damage to the
767 mtDNA. **e -g** (-WI, n=20; +AMS, n=5; +WI, n= 24; +DMM, n= 4) **h** (Cont, n=8; -WI,
768 n=4; +AMS, n=5; +WI, n= 7; +DMM, n= 8). Data are means ± SEM). * P < 0.05, **P <
769 0.01, ****P < 0.0001 by one-sided unpaired t-test with Welch's correction.

Figure 1

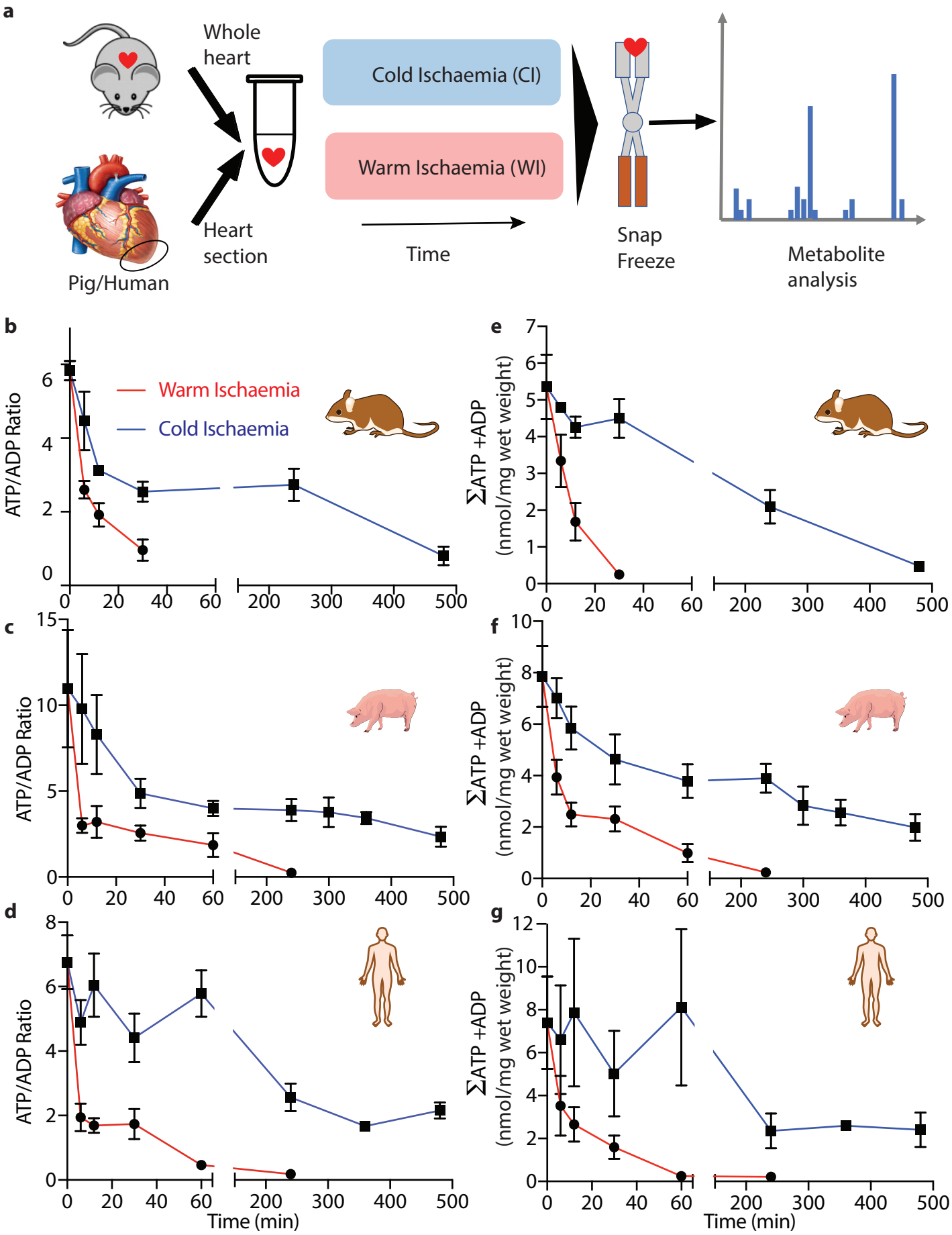
a
Whole heart
Heart section
Pig/Human
Cold Ischaemia (CI)
Warm Ischaemia (WI)
Time
Snap Freeze
Metabolite analysis
b
ATP/ADP Ratio
Warm Ischaemia
Cold Ischaemia
e
ΣATP +ADP (nmol/mg wet weight)
c
ATP/ADP Ratio
f
ΣATP +ADP (nmol/mg wet weight)
d
ATP/ADP Ratio
Time (min)
g
ΣATP +ADP (nmol/mg wet weight)
Time (min)

Figure 2

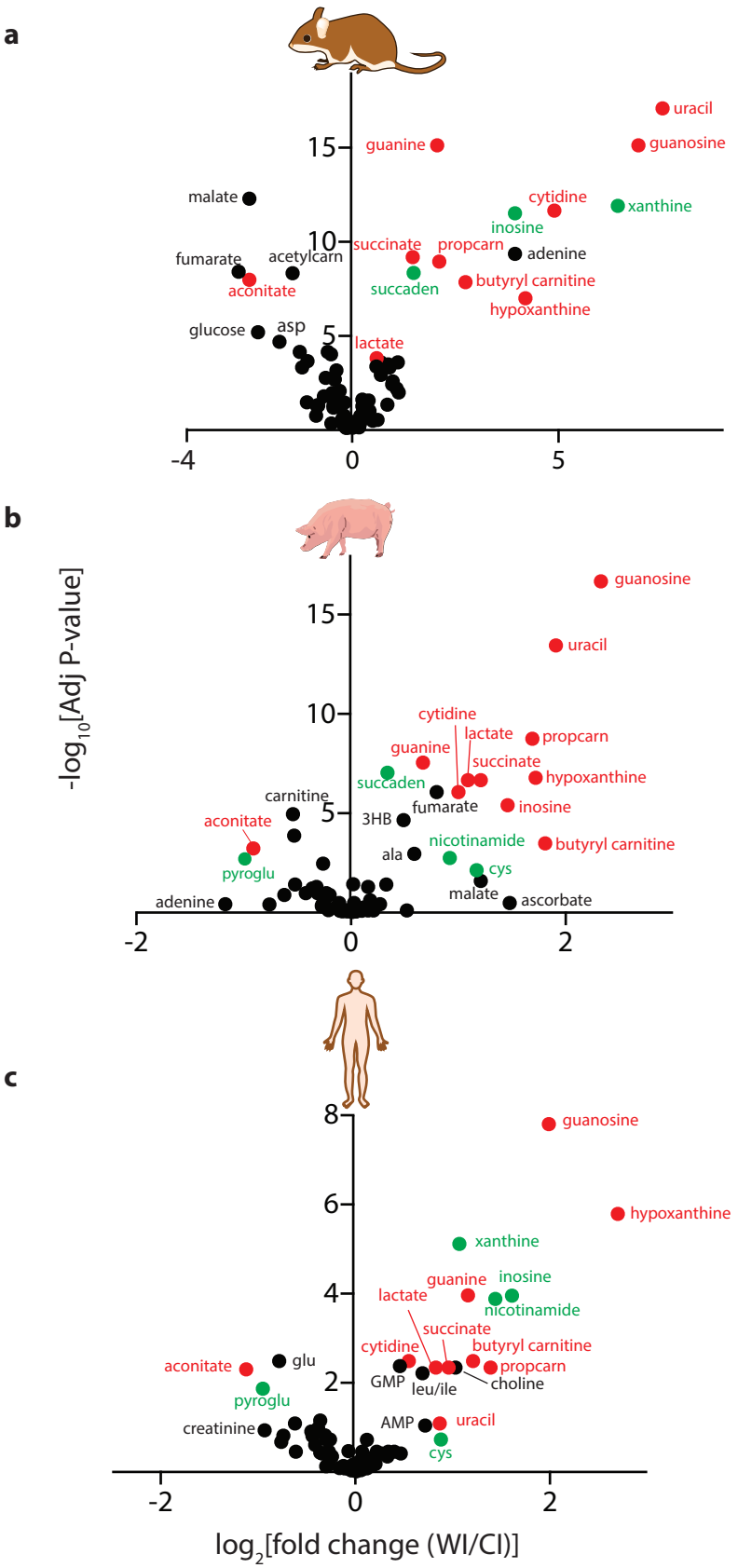
a
uracil
guanosine
guanine
malate
cytidine
xanthine
inosine
succinate
propcarn
adenine
fumarate
acetylcarn
succaden
butyryl carnitine
aconitate
hypoxanthine
glucose
asp
lactate
15
10
5
-4
0
5
b
guanosine
uracil
cytidine
lactate
propcarn
guanine
succinate
succaden
hypoxanthine
carnitine
fumarate
inosine
3HB
aconitate
nicotinamide
butyryl carnitine
ala
cys
pyroglu
malate
adenine
ascorbate
-log10[Adj P-value]
15
10
5
-2
0
2
c
guanosine
hypoxanthine
xanthine
guanine
inosine
lactate
nicotinamide
succinate
cytidine
butyryl carnitine
aconitate
glu
propcarn
GMP
leu/ile
choline
pyroglu
creatinine
AMP
uracil
cys
8
6
4
2
-2
0
2
log2[fold change (WI/CI)]

Figure 3

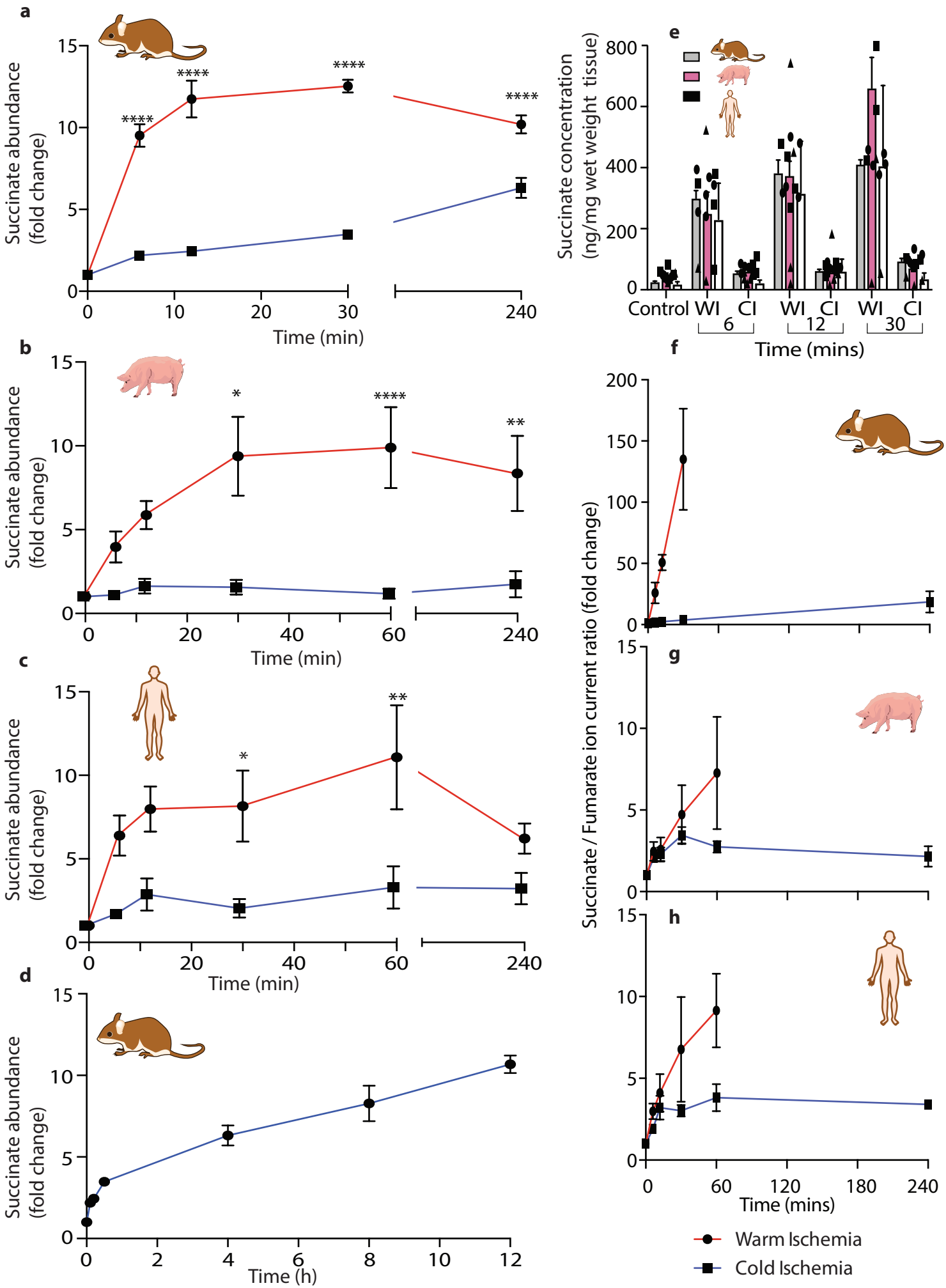
a
Succinate abundance (fold change)
Time (min)
****
b
Succinate abundance (fold change)
Time (min)
*
****
**
c
Succinate abundance (fold change)
Time (min)
*
**
d
Succinate abundance (fold change)
Time (h)
e
Succinate concentration (ng/mg wet weight tissue)
Control
WI
CI
6
12
30
Time (mins)
f
g
h
Succinate / Fumarate ion current ratio (fold change)
Time (mins)
Warm Ischemia
Cold Ischemia

Figure 4

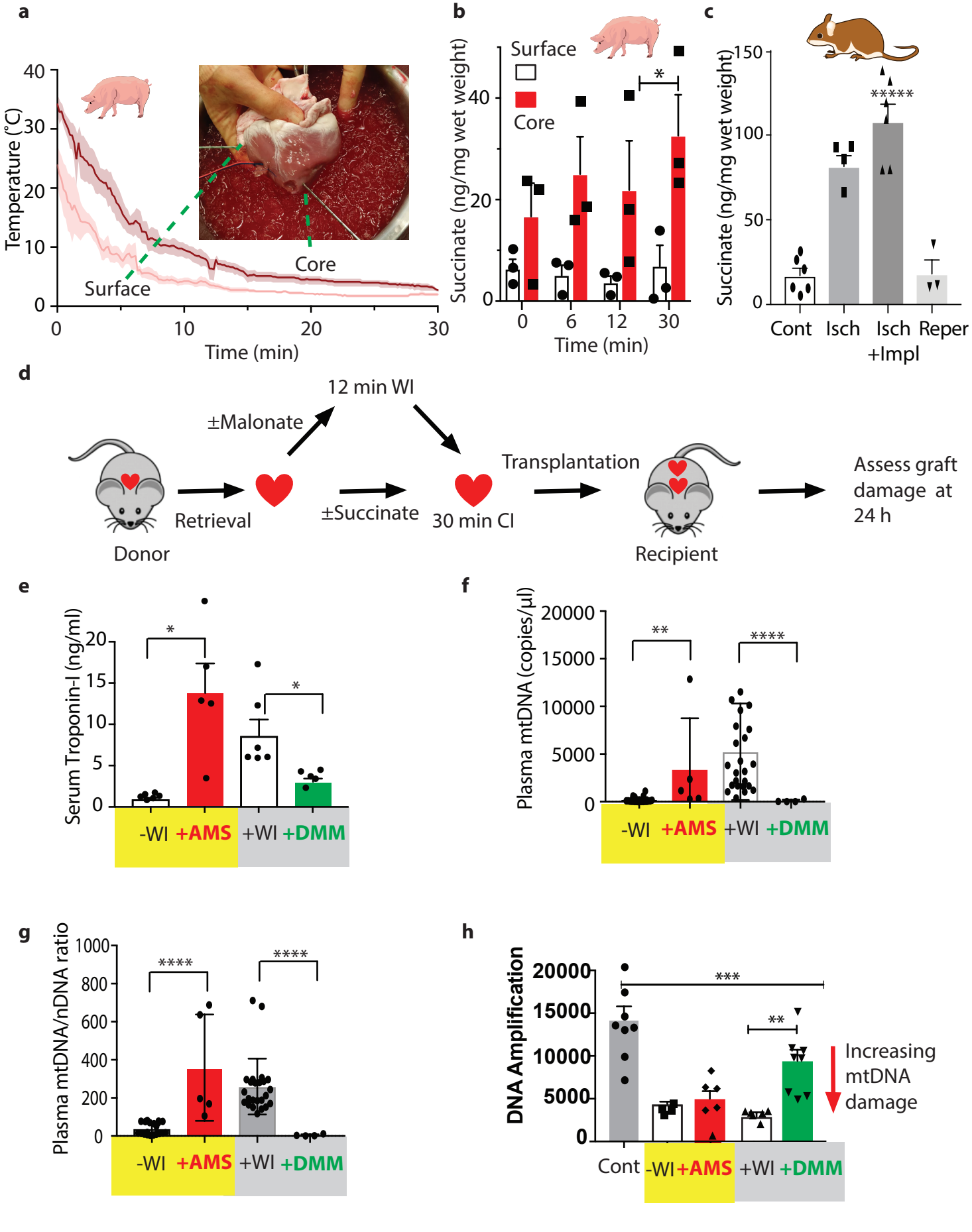
a
Temperature (°C)
Time (min)
Surface
Core
b
Surface
Core
Succinate (ng/mg wet weight)
Time (min)
c
Succinate (ng/mg wet weight)
Cont
Isch
Isch +Impl
Reper
d
12 min WI
±Malonate
Retrieval
±Succinate
30 min CI
Transplantation
Donor
Recipient
Assess graft damage at 24 h
e
Serum Troponin-I (ng/ml)
-WI
+AMS
+WI
+DMM
f
Plasma mtDNA (copies/µl)
g
Plasma mtDNA/nDNA ratio
h
DNA Amplification
Increasing mtDNA damage
Cont

Supplementary Figure 1

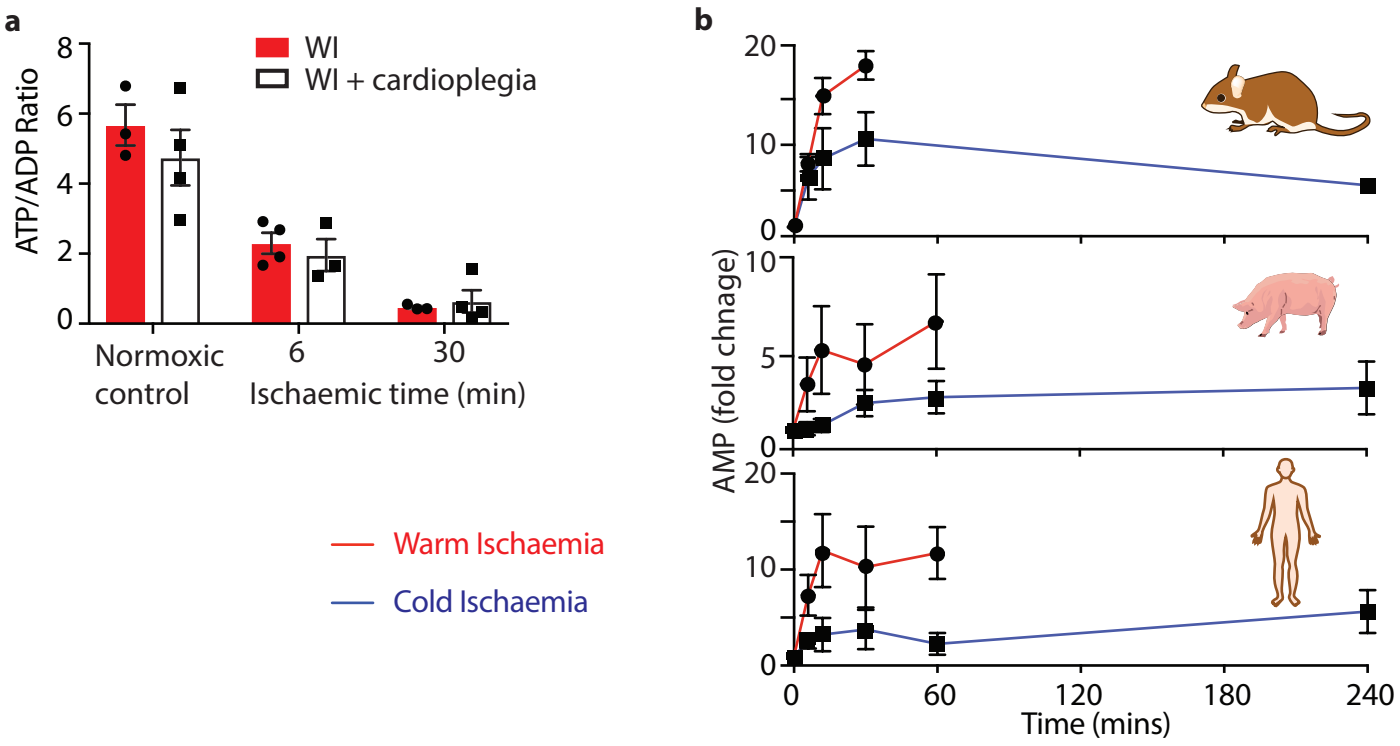

Supplementary Figure 2

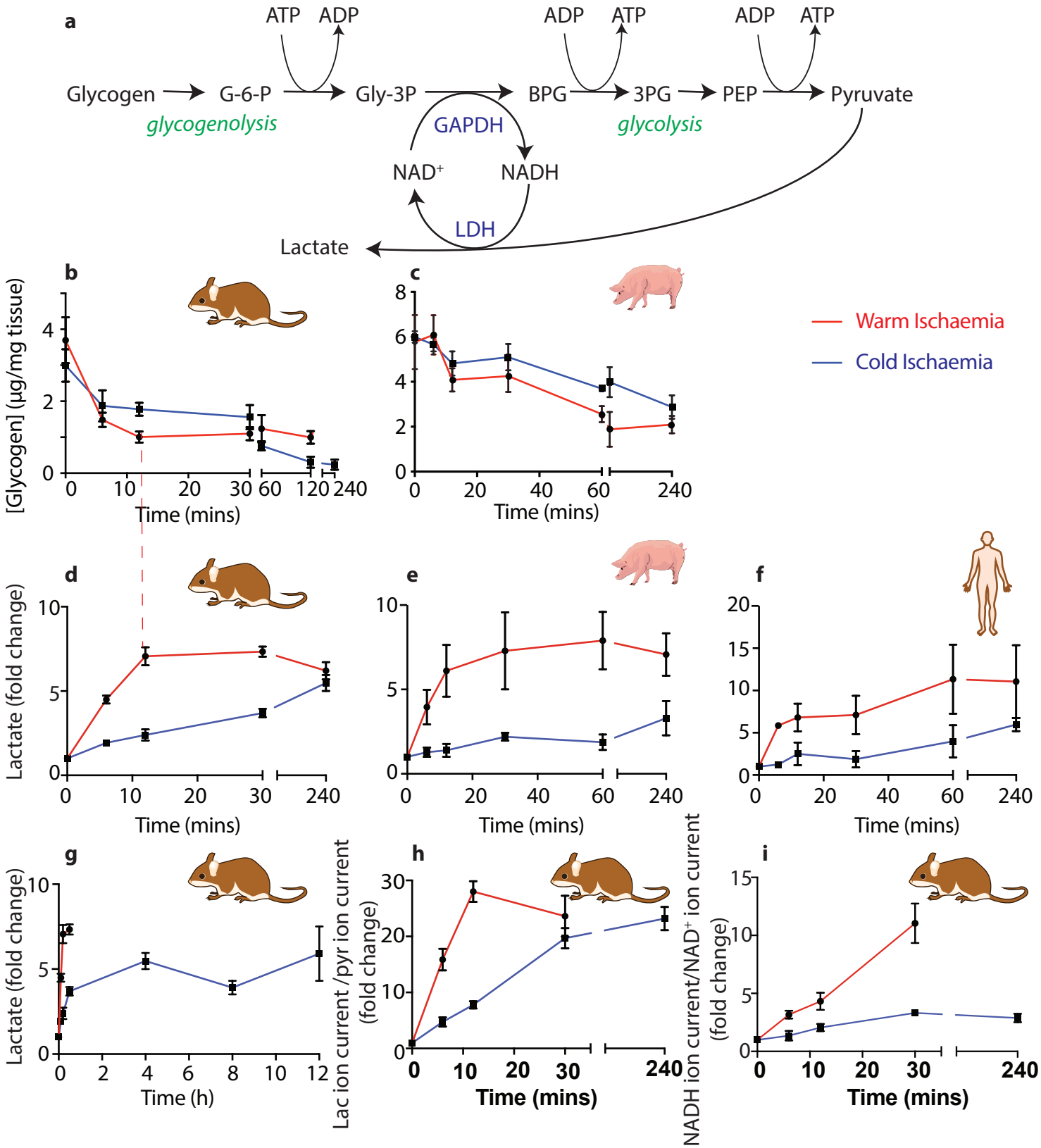

Supplementary Fig 3

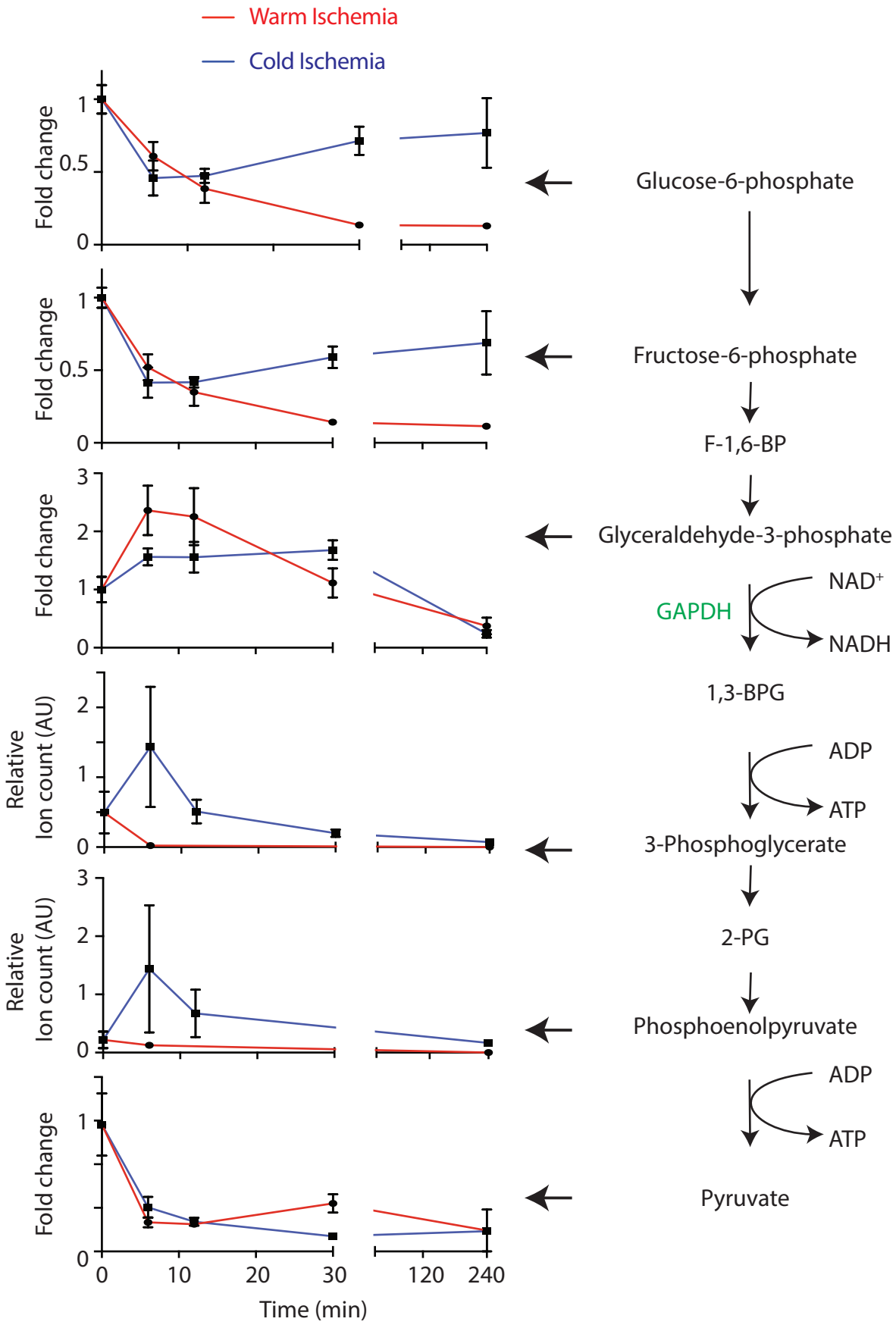

Supplementary Figure 4

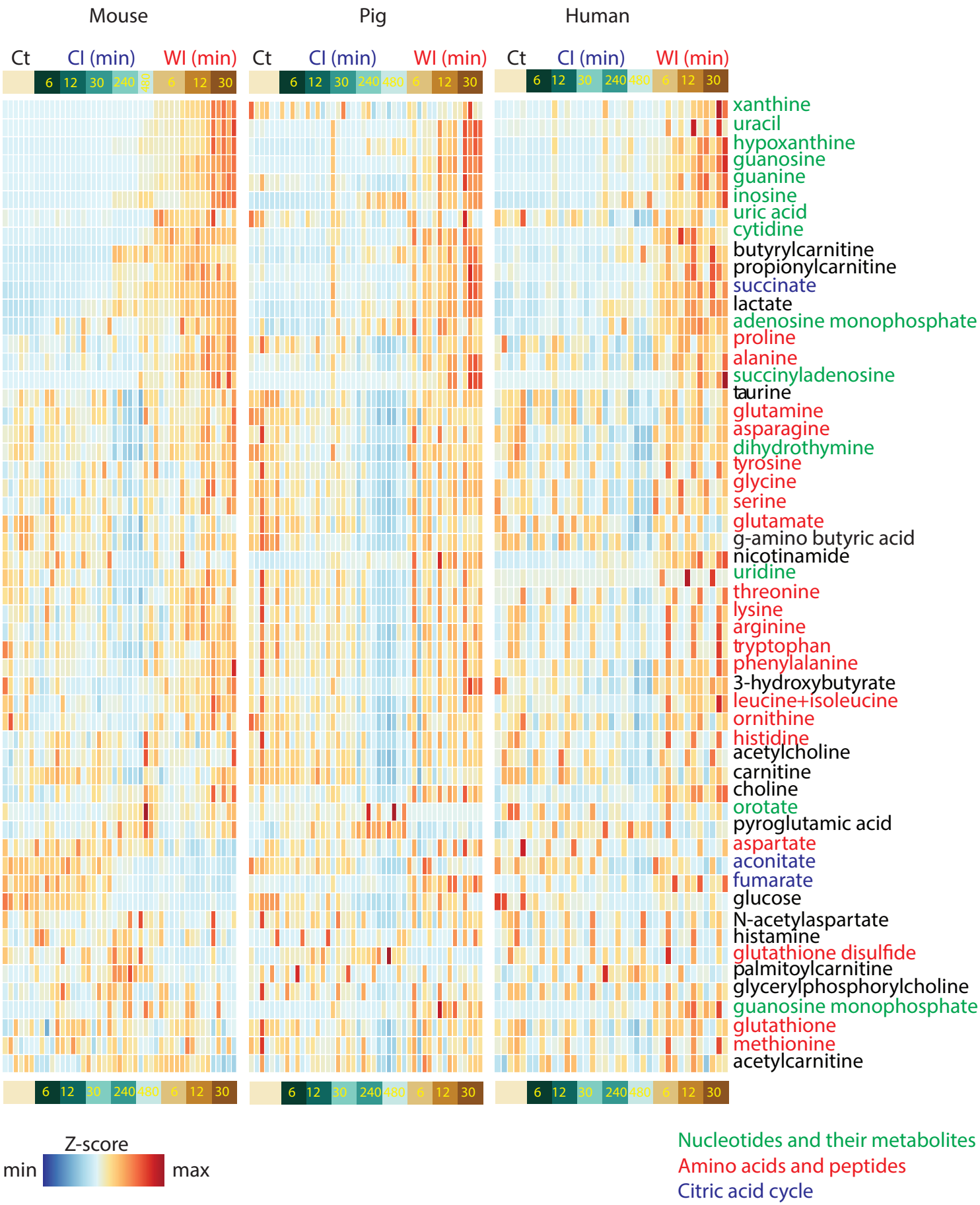

Supplementary Fig 5

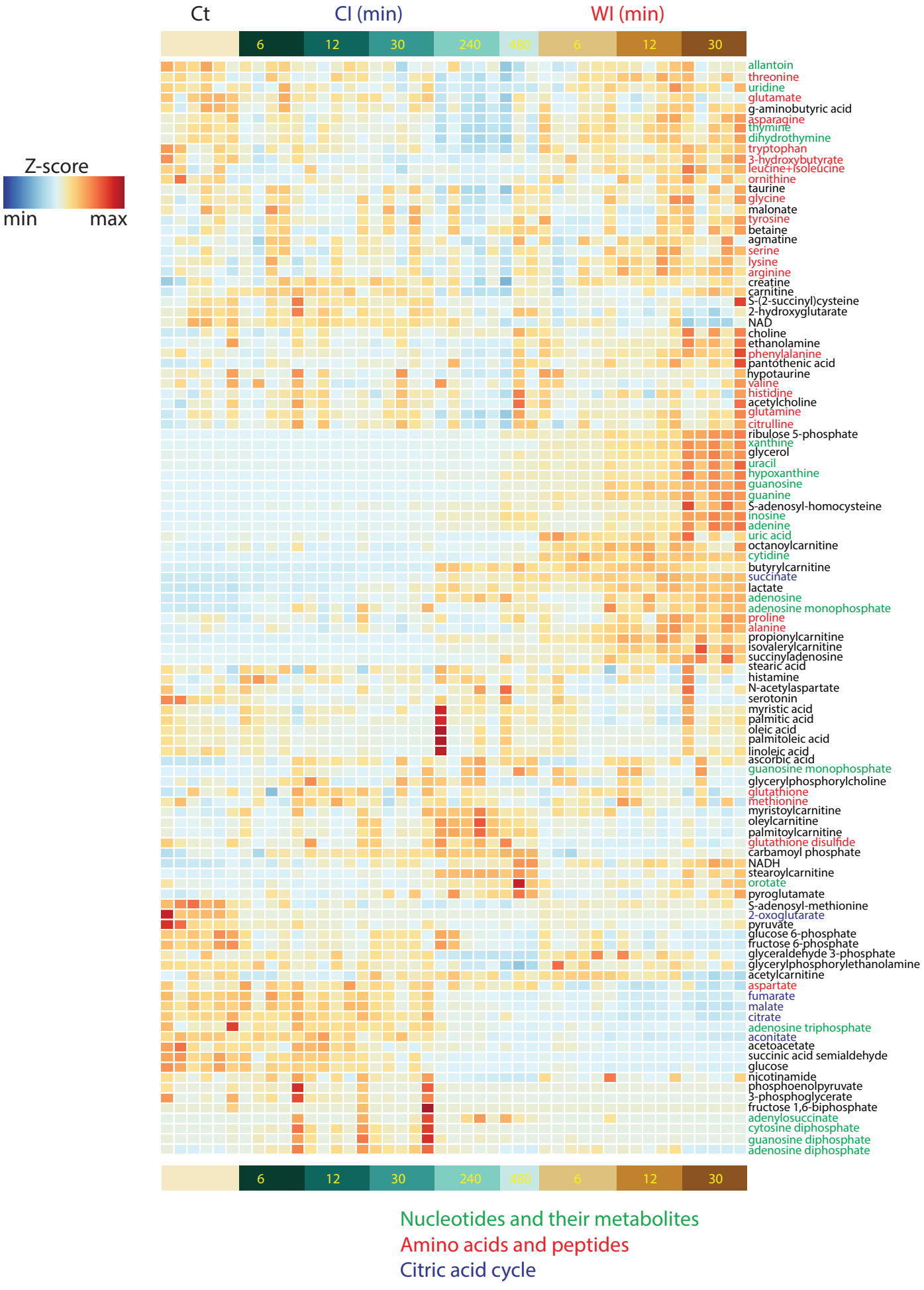

Supplementary Fig 6

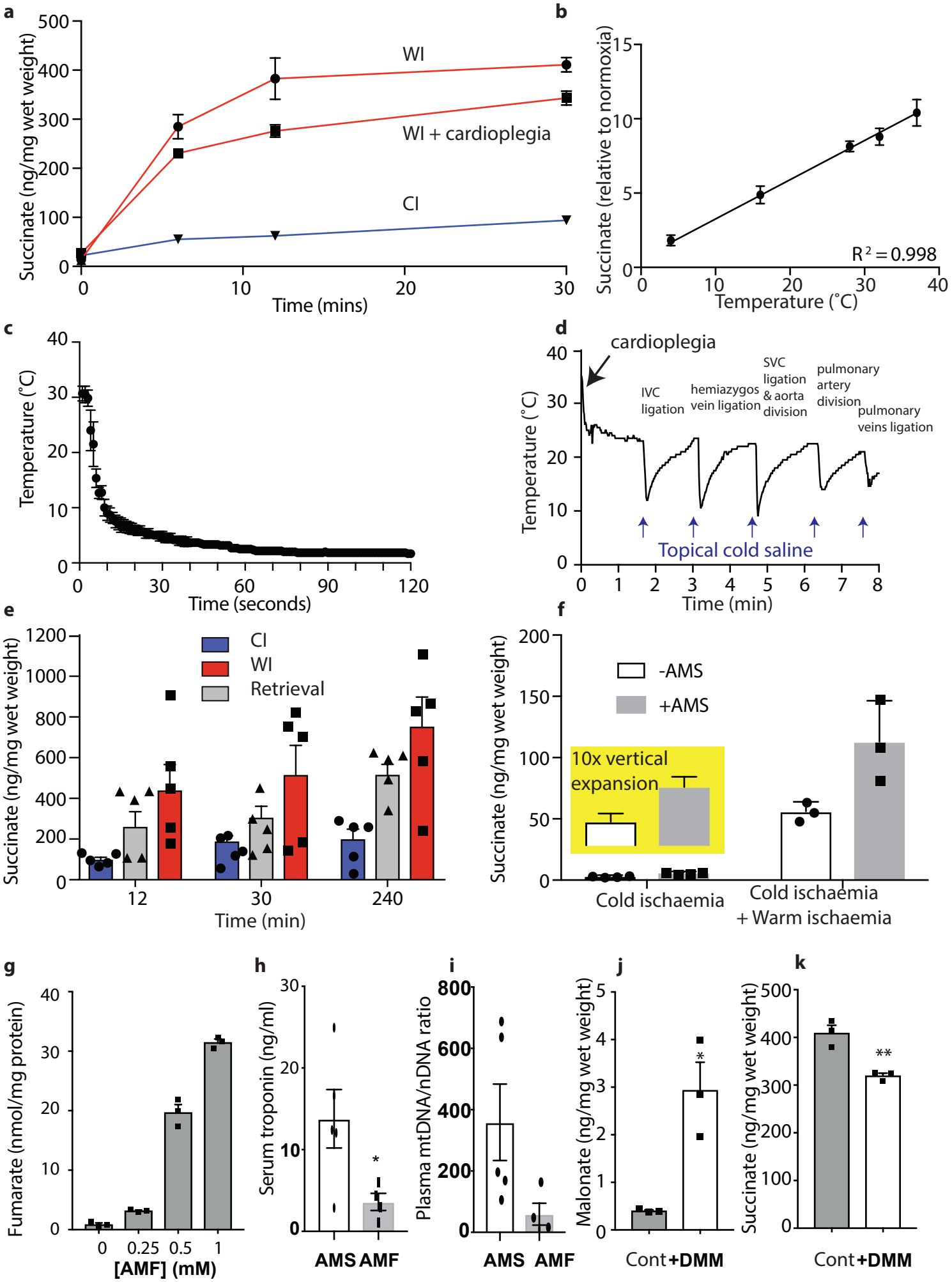

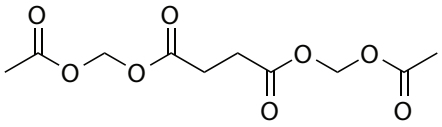

Bis(acetomethoxy)succinate

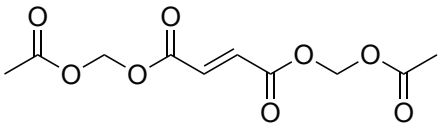

Bis(acetomethoxy)fumarate